

# DETECTION AND MEASUREMENT OF FATIGUE STATE IN FERROMAGNETIC AND AUSTENITIC STEELS USING EDDY CURRENT SENSORS ARRAYS

R. Grimberg<sup>1</sup>, A. Savin<sup>1</sup>, L. Udpa<sup>2</sup>, S. Udpa<sup>2</sup> and R. Steigmann<sup>1</sup>

<sup>1</sup>*Nondestructive Testing Department, National Institute of Research and Development for Technical Physics, 47 D. Mangeron Blvd., Iasi 700050, Romania*

<sup>2</sup>*Department of Electrical and Computer Engineering, Michigan State University, 2120 Engineering Building, East Lansing, MI 48824-1226*

## *Abstract:*

*To evaluate fatigue state of austenitic and ferromagnetic steels a sensors array was developed. The studied samples had different degree of fatigue damage until the state of fatigue cracks. The resolution of sensors array was improved using maximum likelihood procedure. To determine the weight vector, the forward problem was solved, using dyadic Green's functions for layered media.*

## INTRODUCTION

The development of advanced diagnostic systems that are able to identify and detect material degradation in the microstructures of steels is a new challenge for non-destructive evaluation. The detection of material degradation due to mechanical and/or thermal fatigue can contribute to the increase of exploitation reliability of pieces and metallic structures as well as to life-time management of certain components [1], [2].

Lifetime extension of nuclear power plants has become an important topic and resulted in the requirement for advanced safety management tools [3]. The appearance and development of martensite phase, ferromagnetic phase that crystallizes in cubic body centred lattice, are specifically to fatigue phenomenon. In the case of austenitic steels (the austenite is a paramagnetic phase that crystallize in cubic face centred lattice) the appearance and development of martensite leads to modification of magnetic permeability of zones that present fatigue phenomenon due to cyclical loading exceeding a specified threshold [4].

Ferromagnetic steels rarely are in mono-phase state. In the case of biphasic ferrite-perlite steels, the fatigue phenomena are accompanied by the increase of ferrite phase concentration in the detriment of perlite one. This leads to local modification of magnetic permeability, too [2].

These components of fatigue-subdued steels make possible the using of electromagnetic methods to evaluate pre-cracking damage state as well as the detection of fatigue cracks. The fatigue state evaluation is made through metallography procedures and by X ray diffraction.

### Materials and test conditions; EDDY CURRENT SENSORS ARRAY

The investigations were performed on specimens according to ASTM E606, (Fig. 1).

The studied materials were AISI 304 (austenitic steel) and SAE 4130 (ferromagnetic steel) having the chemical composition given in Table 1. The fatigue tests were performed with alternating loading with a test frequency of 2 Hz at room temperature.



**Fig 1. The specimen**

The amplitude of loading was 150MPa. From each material type, 5 samples were performed.

**Table 1. Chemical composition [%wt]**

Steel	C	Mn	Si	P	S	Ni	Cr	Mo
AISI 304	0.08	2.0	1.0	0.045max	0.03max	8.0-10.5	18-20	-
SAE 4230	0.4	0.75	0.2	0.04max	0.03max	-	1.1	0.25

The samples were electrochemically skived to wear off the eventually oxide track. Metallography analyses by standard procedure [5] were effect, as well as X ray diffraction using  $MoK_{\alpha}$  radiation. The fatigue cracks were emphasized using penetrant liquid [6].

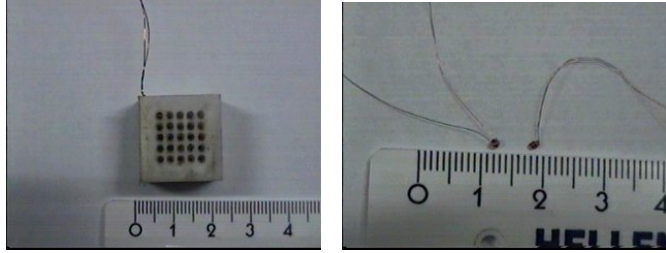


**Fig.2. Eddy current sensor array general view&reception coils**

For the fatigue state evaluation and cracks emphasizing the eddy current sensors array used is a send – receiver type [7], [8], [9].

The emission part is made from one coil with 20x20mm dimensions, having 100 turns. The reception part is made from 5x5 identical coils having each outer diameter 2mm, the distance between the centers of

coils being 2.4mm, Figure 2. The connection of array to the measurement equipment is presented in [2].

### SIGNAL PROCESSING SCHEME

Applying the sensors array on AISI 304 sample, the response of reception coils that form the array, presented in Figure 3, is obtained. The current frequency was 10KHz and amplitude 0.1A. Placing the array on a plate from the same material, that present 2 hole with flat bottom, having 1mm diameter and 1mm depth, disposed so that they are placed under the center of the reception coils (5,2) and (4,4) (the number from brackets represent the position of sensor in array), the response signal presented in Figure 4 is obtained. The resolution of eddy current sensors array can be substantial improved using super-resolution procedures, similarly with those developed for radar and sonar [10]. To correctly localize the material discontinuities and the magnetic permeability modifications, the array manifold should be free of ambiguity [9].

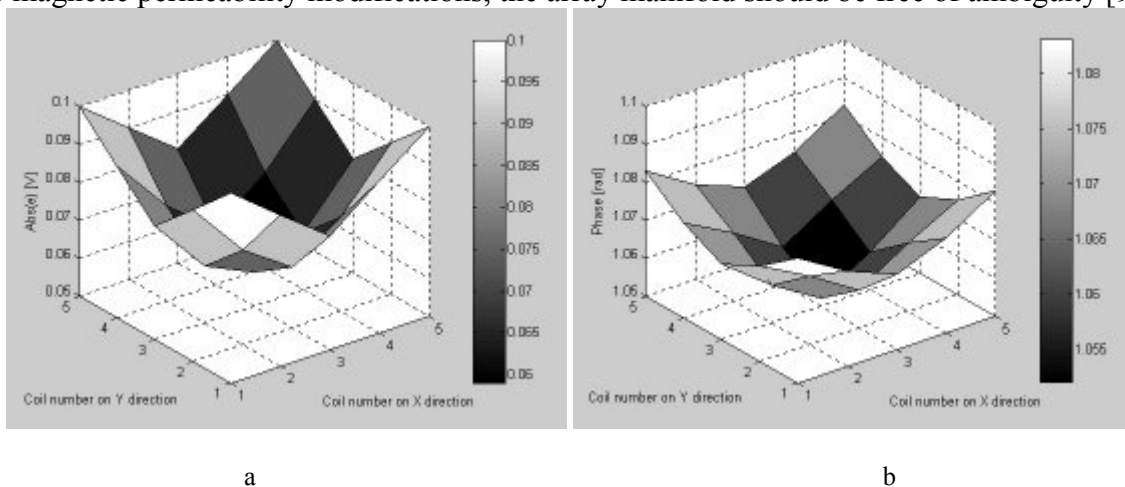


**Fig 3. Amplitude (a) and phase (b) of induced electromotive force recorded by each of receiving coils; the sensors array is placed on AISI 304 sample without fatigue**

Any trace of ambiguity can be removed using weight vector  $\bar{w}$ , which makes a linear combination of the output signal from the sensor array into a single output signal  $\bar{y}$

$$\bar{y} = \bar{x}w^H \quad (1)$$

where superscript H denotes the Hermitic operation (i.e. conjugate-transpose).

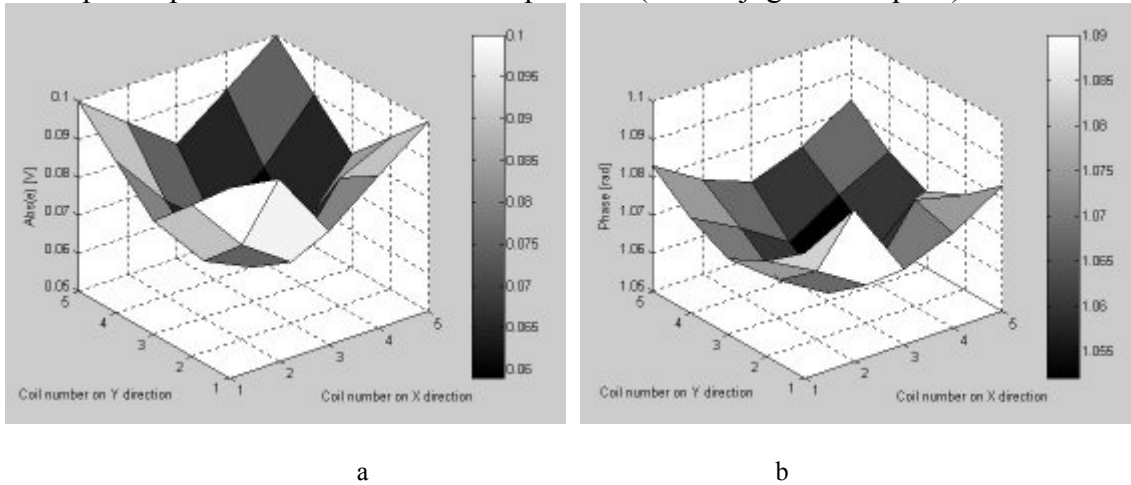


**Fig 4. Amplitude (a) and phase (b) of induced electromotive force recorded by each of receiving coils. 2 holes with flat bottom are placed under coils (5,2) and (4,4)**

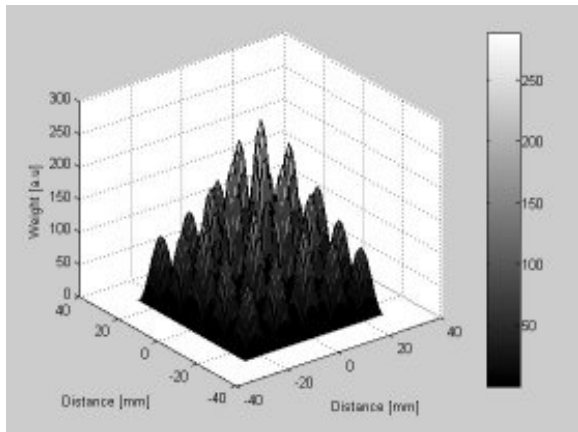


**Fig 5. Matrix of weight vectors**

To eliminate the 1<sup>st</sup> order ambiguities, [10], we have considered, ideally, that the sensitivity distribution for one sensor from array satisfies a cosines rule, i.e. is maximum in center and null on reception coil border. With this aim, the surface of a coil was discretized in 10x10 intervals. The sensitivity in the center of a coil depends on their position and the amplitude and frequency of the current through emission coil when the array is placed on a isotropic and homogeneous region of material.

In Figure 5 is presented the matrix of the weight vectors for the case in which under the center of coil (1,1) is a bottom flat hole.

To determine the position of discontinuities and magnetic permeability modifications, we use a super-resolution method based on the maximum likelihood procedure [11].

In this method, the positions of discontinuities and of zones with magnetic permeability modifications are given by the maximum of product  $SR_{xx}$  where  $R_{xx}$  is auto-correlation matrix

$$R_{xx} = xx^H \quad (2)$$

and S is defined by

$$S = A(A^H A)^{-1} A^H \quad (3)$$

with array's sensitivity matrix  $A = ww^H$  applying the procedure described above, the fatigue cracks that appear after  $8 \times 10^5$  cycles on AISI 304 sample and that is presented in Figure 6, being emphasized with penetrant liquid [6], are perfect visible with the array sensor (Fig. 7).

For all possible locations of discontinuities and magnetic permeability modifications the weight vectors must be constructed. The single method possible to be used is the solving of forward problem for the sensor array. After  $7.5 \times 10^5$  cycles, for samples made from AISI 304,

damage factor had 0.8 value. In Figure 8 is presented the response of array in this situation and in Figure 9 the variation of martensite content in the length of sample.

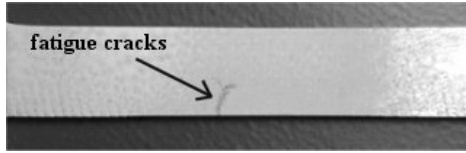


Fig 6. Fatigue cracks on AISI 304 sample;

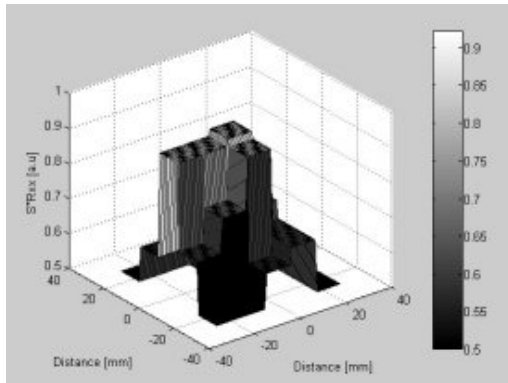


Fig.7. Sensor array response

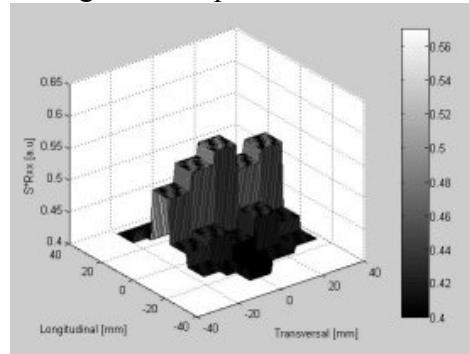


Fig 8. Sensor array response;

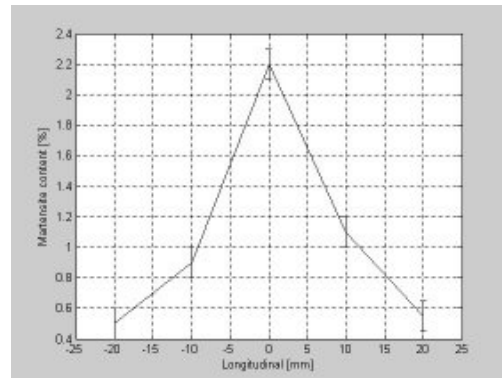


Fig. 9. Distribution of martensite content along sample's length

### Sensors array functioning model

To model the functioning of sensors array, the dyadic Green's function [12] and volume integral methods were used. The field in material, created by emission part of array, rectangular, with  $2a \times 2b$  dimensions and  $\epsilon_1 \times \epsilon_2$  section having  $N_s$  turns, through which an current with  $\omega$  angular speed and  $I_0$  amplitude circulates, will be

$$\vec{E}_0(\vec{r}) = j\omega\mu_2 \int_{V_{source}} \vec{G}_{12}(\vec{r}, \vec{r}') \vec{J}(\vec{r}') d\vec{r}' \quad (4)$$

where  $\vec{J}$  is given in [13]. The frame being parallel with examined surface, the created field will be transversal electric (TE), the calculus being made in Cartesian coordinate system. When the examined object is flat, with finite width, the expression of  $\vec{G}_{12}$  dyad in Fourier space is

$$\vec{G}_{12} = \frac{j}{8\pi^2} \begin{pmatrix} k_y^2 & -k_x k_y & 0 \\ -k_x k_y & k_x^2 & 0 \\ 0 & 0 & 0 \end{pmatrix} F_-(z, z') \frac{1}{k_{1z} k_s^2} \exp(jk_x(x-x') + jk_y(y-y')) \quad (5)$$

where

$$F_-(z, z') = \left[ e^{-jk_2 z z'} + e^{jk_2 z(z+2d_2)} \tilde{R}_{23} \right] e^{jk_2 z d_1} \tilde{T}_{12} e^{-jk_2 z d_1} e^{jk_1 z z'} \tilde{M}_2 \quad (6)$$

with  $\tilde{M}_2 = \left[ 1 - \tilde{R}_{23} \tilde{R}_{21} e^{2jk_2 z(d_2-d_1)} \right]^{-1}$  ;

$k_{1z} = (k_1^2 - k_s^2)^{1/2}$ ;  $k_{2z} = (k_2^2 - k_s^2)^{1/2}$ ;  $k_1^2 = \omega\mu_1 \left( \varepsilon_1 + j \frac{\sigma_1}{\omega} \right)$ ;  $k_2^2 = \omega\mu_2 \left( \varepsilon_2 + j \frac{\sigma_2}{\omega} \right)$ ,  $\tilde{T}_{12}$  and  $\tilde{R}_{23}$  being generalized transmission and respective reflexion coefficients [12],  $d_1$  is the distance from plane XOY to superior face of material and  $d_2$  to inferior face.

The interest zone from material is discretized in  $N_x \times N_y \times N_z$  identical cells with  $\Delta x \times \Delta y \times \Delta z$  dimensions, small enough so the field in the center of cell is, in fact, the field in cell. The equations are discretized through moment method, point-matching variant.

The presence of material discontinuities is equivalent with an auxiliary source that creates the field described by dyadic Green's function  $\tilde{G}_{22}(\bar{r}, \bar{r}')$ . Due to TE character of the field, the dyad  $\tilde{G}_{22}(\bar{r}, \bar{r}')$  won't present discontinuities, so that the integrals on defect's volume will be well defined.

In Fourier space, the dyad  $\tilde{G}_{22}(\bar{r}, \bar{r}')$  is

$$\tilde{G}_{22} = \frac{j}{8\pi^2} \begin{pmatrix} k_y^2 & -k_x k_y & 0 \\ -k_x k_y & k_x^2 & 0 \\ 0 & 0 & 0 \end{pmatrix} F_{\pm}(z, z') \frac{1}{k_{2z} k_s^2} \exp(jk_x(x-x') + jk_y(y-y')) \quad (7)$$

where

$$F_+(z, z') = \left[ e^{-jk_{2z}z'} + e^{jk_{2z}(z'+2d_2)} \tilde{R}_{23} \right] \left[ e^{jk_{2z}z} + e^{-jk_{2z}(z+d_2)} \tilde{R}_{12} \right] \tilde{M}_2 \text{ for } z > z'$$

$$F_-(z, z') = \left[ e^{jk_{2z}z'} + e^{-jk_{2z}(z+2d_1)} \tilde{R}_{21} \right] \left[ e^{-jk_{2z}z} + e^{jk_{2z}(z+d_2)} \tilde{R}_{23} \right] \tilde{M}_2 \text{ for } z < z'$$

The dyad  $\tilde{G}_{22}$  was analytical integrated on the cell's volume. For the case  $z=z'$ , the punctual value is given by

$$\int_{z_p + \frac{\Delta z}{2}}^{z'} G_{22lm}^+ dz' + \int_{z'}^{z_p + \frac{\Delta z}{2}} G_{22lm}^- dz' \quad (8)$$

where  $z_p$  is  $z$  coordinate of the  $p$  cell's center,  $l, m \in \{x, y, z\}$ ,  $G_{22lm}^+$  is the expression for  $z > z'$  and  $G_{22lm}^-$  for  $z < z'$ .

In the presence of a discontinuity in material with  $\sigma_f$ , the field in material will be

$$\bar{E}_2(\bar{r}) + j\omega\mu_2\sigma_2 \int_{V_{flaw}} \tilde{G}_{22}(\bar{r}, \bar{r}') \bar{E}_2(\bar{r}') \left[ \frac{\sigma_f(\bar{r}')}{\sigma_2} - 1 \right] d\bar{r}' = \bar{E}_0(\bar{r}) \quad (9)$$

To obtain  $\bar{E}_2(\bar{r})$ , the discretized variant of Fredholm equation was solved using the inverse in More-Penrose sense. The field scattered in air by discontinuity is

$$\bar{E}_1(\bar{r}) = j\omega\mu_2\sigma_2 \int_{V_{flaw}} \tilde{G}_{21}(\bar{r}, \bar{r}') \bar{E}_2(\bar{r}') \left[ \frac{\sigma_f(\bar{r}')}{\sigma_2} - 1 \right] d\bar{r}' \quad (10)$$

and the induced electromotive force in one reception coil will be given by the circulation of  $\bar{E}_1(\bar{r})$ . The expressions of  $\tilde{G}_{21}$  components are obtained by similar procedures.

To obtain the weight vectors  $\bar{w}$ , it were imagined different positions of discontinuity in material, calculating every time the array's response.

To obtain the weight vectors in the case of local modification of permeability due to fatiguing of samples submitted to cyclical loading, it was proceed in a simple way with the note that to report  $\frac{\sigma_f(\bar{r}')}{\sigma_2}$ , 1.001 value was attributed and to  $\mu_2$  in the region of martensite phase

appearance  $5\mu_0$  value was assigned. In the case of ferrite phase increasing,  $\mu_2$  in un-fatigued material has  $800\mu_0$  value and in the zone subdued to fatigue, respective  $850\mu_0$ .

## CONCLUSIONS

To determine the fatigue damage to austenitic and ferromagnetic steels, a send-receiver type eddy current sensors array was developed. The method is based on experimental observation that the fatigue leads to the appearance of martensite phase at austenitic steels and to increasing of ferrite concentration at bi-phases ferrite-perlite steels.

The using of maximum likelihood procedure permits to clearly emphasize the shape and position of fatigue cracks as well to fatigue damage. The obtained results are in good concordance with the examination with penetrant liquids and with those obtained by X ray diffraction.

The developed theoretical model, based on dyadic Green's function for planar-layered media has allowed the determination weight vectors for diverse shapes, natures and positions of zones with different fatigue damages.

## ACKNOWLEDGMENTS

*This work was partially supported by US NSF Grant #0303914 and CNCSIS –Romania under Grant No.982/2004.*

## References

1. Rontola R., "Thermal Fatigue Experiences Countermeasures in Finland", Report IAEA TC 485.27 (1991)
2. Grimberg R., Savin A., Leitoiu S. and Craus M.L., *INSIGHT*, 38, 9, (1996),p. 650-655
3. Ebine N., Suzuki M. and Ara K., "Nondestructive measurement to evaluate changes of material properties of ferromagnetic structural steels with planar coils", *Studies in Applied Electromagnetics and Mechanics*, 21, Electromagnetic Nondestructive evaluation (V), eds. J.Pavo, G.Vertesy, T.Takagi and S.S. Udpa, IOS Press (2001), p. 283-290
4. Lemaitre J. and Chaboche J.L., *Mechanics of Solid Materials*, Cambridge University Press, NY, (1994)
5. Honeycombe R.W.K., *Steels, Microstructures and Properties*, Edward Arnold Publishers Ltd. (1981)
6. Lovejoy D., *Penetrant Testing*, Chapman&Hall, London, (1991)
7. Auld B.A., in *Review of Progress in QNDE*, vol. 10, eds. D.O.Thomson, D.E.Chimenti, Plenum Press, New York, (1991), p.951-955
8. Hurley D.C., Hedengren K.H. and Young J.D., in *Review of Progress in QNDE*, vol. 11, *op.cit.*(1992), p.1137-1144
9. Grimberg R.Wooh S.C., Savin A., Steigmann R. and Premel D., *INSIGHT*, 44, 5, (2002), p.289-293
10. Shell S.V. and Gardner W.A., "High Resolution Direction Finding", *Handbook of Statistics*, vol.10, eds. N.K.Bose, C.R.Rao, Elsevier, Amsterdam, 1993,p.755-817
11. Zhao L. Krishnaiah P. and Boi Z., *J.Mutivariate Anal*, 20, (1986), p.1-25
12. Chew W.C., *Waves and Fields in Inhomogeneous Media*, Van Nostrand Reinhold, NY, (1990)
13. Grimberg R., Savin A., Radu E., Mihalache O., *IEEE Trans on Mag.*, 36, 1, (2000), 299-307